

# NEAR-SUN SOLAR WIND CONSEQUENCES OF SOLAR STRUCTURE AND DYNAMIC PHENOMENA OBSERVED BY RADIO SCINTILLATION MEASUREMENTS

Richard Woo

*California Institute of Technology, Jet Propulsion Laboratory, Pasadena, California, USA*

## ABSTRACT

Since radio propagation measurements using either natural or spacecraft radio signals are essentially our only means for probing the solar wind in the vicinity of the Sun, they represent a key tool for studying the interplanetary consequences of solar structure and dynamic phenomena. While such measurements have been actively pursued over the past forty years, significant new information on the near-Sun consequences has recently been obtained from radio scintillation observations of coherent spacecraft signals. This paper reviews results covering density fluctuations, fractional density fluctuations, coronal streamers, heliospheric current sheets, coronal mass ejections and interplanetary shocks. An unprecedented opportunity to carry out joint ICE S-band (13 cm wavelength) Doppler scintillation measurements with the SOHO white-light coronagraph (1. ASCO) is also described.

**Keywords:** Radio scintillation, compressive fluctuations, coronal streamers, coronal mass ejections, heliospheric current sheet.

## I. INTRODUCTION

Observations of the solar wind close to its source and before evolution are crucial for understanding the interplanetary consequences of solar structure and dynamic phenomena. Because no direct spacecraft measurements have been made inside 0.3 AU, most of our information on solar wind properties and their variations in this dynamically interesting region have come from remote sensing radio propagation measurements.

When a radio wave propagates through the solar wind, scattering by the ubiquitous electron density fluctuations gives rise to a host of radio scattering phenomena that can be observed with natural radio sources or spacecraft radio signals. These observations, which include angular broadening, intensity scintillation (termed IPS for interplanetary scintillation), Doppler (or equivalently phase) scintillation, spectral broadening, frequency decorrelation, have been used over the past four decades to probe the solar wind inside 0.3 AU (Ref. 1-4) and are referred to collectively in this paper as radio scintillation measurements.

Recent advances, mainly with Doppler scintillation measurements, have made it abundantly clear that substantial variation in density fluctuations takes place in the vicinity of the Sun (Ref. 5,6). These results

underscore the value of measurements that sense density fluctuations for investigating the interplanetary consequences of solar structure and events, particularly when conducted in conjunction with solar observations such as those of white-light and soft X-rays. The purpose of this paper is to review and place into perspective the latest results on near-Sun solar wind structure, both quasi-static and dynamic. A unique opportunity for carrying out future joint ICE scintillation and SOHO white-light measurements is also described.

## 11. BACKGROUND

Radio scintillation investigations of the solar wind near the Sun, which yield information on electron density fluctuations and solar wind speed, have been carried out first with natural radio sources and later also with spacecraft radio signals. The earliest experiments observed angular broadening of natural radio sources, and determined the radial dependence of density fluctuations  $\delta n_e$  (and consequently electron density  $n_e$  under the assumption that it is proportional to  $\delta n_e$ ) (Ref. 7-10). Interestingly enough, these took place even before the existence of the solar wind was confirmed by Mariner 2 plasma measurements in 1962. More recent angular broadening measurements (Ref. 11) have revealed high anisotropies of the density irregularities inside a few solar radii, while longer baseline measurements have yielded information on larger spatial scales (Ref. 12). Additional properties of the density fluctuations obtained include their dependence on latitude and solar cycle (Ref. 13,14) and their spatial wavenumber distribution (Ref. 6,15-19). Spectral broadening measurements of monochromatic spacecraft radio signals have also led to the determination of the latitudinal variation of solar wind speed and mass flux in the acceleration region during solar minimum conditions (Ref. 20), results that have been confirmed by the 1994 Ulysses plasma measurements over the south pole but beyond 2 AU [M. Neugebauer, private communication]. The mass flux measurements are also consistent with results deduced from Lyman- $\alpha$  observations for the solar wind near 1 AU (Ref. 21).

With the discovery of IPS in 1964 (Ref. 22), a means for measuring solar wind speed using multiple observing antennas became available. Near the Sun, IPS measurements showed the acceleration of the solar wind (Ref. 23-26), while beyond 0.5 AU, they revealed the latitudinal variation of solar wind speed and the global distribution of solar wind speed in terms of the large-scale coronal magnetic field (Ref. 27,28).

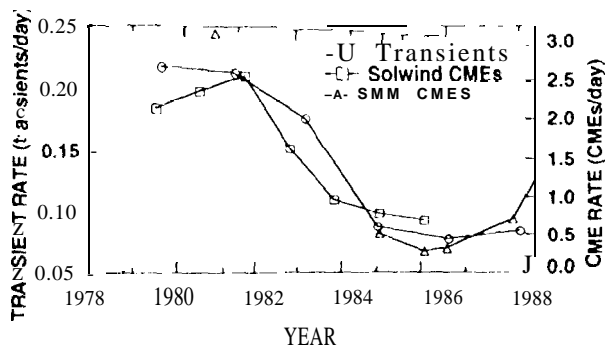


Figure 1. Comparison of Doppler scintillation transient rates with CME rates of Solwind and SMM coronagraph measurements (from Ref. 37)

In addition to characterizing the properties of density fluctuations and solar wind speed, radio scintillation and scattering measurements are useful for studying large scale features manifesting enhancements in density fluctuations and causing scintillation transients. Examples of these include propagating interplanetary disturbances (Ref. 29-33) and leading edges of high-speed streams beyond 0.3 AU (Ref. 34,35). Doppler scintillation measurements, which have a wide dynamic range and high time resolution over extensive heliocentric distances, have been especially effective for detecting transients, many of which are interplanetary shocks (Ref. 3, 1,36). The frequency of occurrence of Doppler scintillation transients, along with corresponding rates of coronal mass ejections observed by Solwind and SMM white-light coronagraphs, covering a solar cycle are shown in Fig. 1 (Ref. 37). The general agreement between the two further strengthens the notion that scintillation and optical transients are different manifestations of the same physical phenomena (Ref. 38).

Time-delay (ranging) and Faraday rotation are two additional radio propagation measurements made with natural and spacecraft radio signals to investigate electron density and magnetic fields in the inner heliosphere near the Sun (Ref. 39-42). Analysis of Faraday rotation fluctuations has provided estimates of magnetic field fluctuations (Ref. 43).

### 11.1. DENSITY FLUCTUATIONS

In spite of the success in probing the solar wind with radio propagation experiments, especially those observing radio scintillation and scattering phenomena, progress in characterizing and understanding the global morphology of the near-Sun solar wind and its relationship to solar or coronal features has been slow. Compared with *in situ* plasma measurements, the volume of radio observations near the Sun is miniscule, because during each experiment observations typically last only a few days. Not only do these radio measurements take place in a short time, but they often span a wide range of latitudes and certainly a wide range of heliocentric distances. Furthermore, because the

radial dependence usually dominates the sparse measurements, radio measurements of the near-Sun solar wind have yielded mainly information on the radial variations of electron density, electron density fluctuations and solar wind speed.

Radio propagation investigations of the inner solar wind entered a new and exciting era with the recent discovery that, near the Sun and before evolution, solar wind structure characterized by density fluctuations is distinctly organized by the large-scale coronal magnetic field (Ref. 5,6). The increase in remote sensing abilities of Doppler scintillation over IPS measurements played an important role, but two other factors contributed significantly. First, the scintillation data analyzed were from the late declining phase of the solar cycle, when the tilt of the solar magnetic dipole with respect to the Sun's rotation axis led to large-scale organization of the solar wind in such a way that alternating regions of high- and low-speed solar wind were observed in the ecliptic plane. The solar wind configuration was, therefore, very similar to that when the connection between high-speed streams and coronal holes was made during the Skylab period (Ref. 44). Second, correlation was facilitated by the fact that the observed variations in Doppler scintillation and hence density fluctuations were often dramatic and abrupt.

The solar wind is organized in such a way that near the neutral line (heliospheric current sheet), where the magnetic fields are predominantly closed and the solar wind is slow, density, density fluctuations, and variability in density fluctuations are all found to be high (Ref. 5). The high variability (presence of enhancements) in density fluctuations in the streamer belt is associated with coronal mass ejections as well as quasi-stationary phenomena such as coronal streamers (Ref. 6). That CMEs often take place in the streamer belt is consistent with conclusions reached in studies of white-light coronagraph measurements (Ref. 45,46). Far from the neutral line — where the magnetic fields are open and the wind is fast — density, density fluctuations, and variability in density fluctuations are all conspicuously low. In terms of quasi-stationary structure, the organization appears broad, taking place over a large portion of the solar cycle.

Possible inconsistencies raised earlier (Ref. 47) between Doppler scintillation measurements close to the Sun and meter wavelength IPS measurements beyond 0.5 AU, have been dismissed by the Doppler scintillation results which span a broad heliocentric distance, range and show evolution of the solar wind. While Doppler scintillation enhancements near the Sun and inside 0.3 AU are associated with the slow wind, beyond 0.5 AU the solar wind evolves to a state distinguished by enhancements at the leading edges of high-speed streams, as observed by meter wavelength IPS measurements (Ref. 5). That the conspicuously quiet Doppler scintillation regions coincide with fast wind regions over coronal holes, provides the clearest evidence yet that these regions are not likely to be the major sources of IPS disturbances observed beyond 0.5

AU (Ref. 48). The Doppler scintillation results also show that the putative permanent region of enhanced density fluctuations (Ref. 13, 49) attributed to the point where the solar wind becomes supersonic is more likely caused by close proximity to the neutral line.

#### IV. FRACTIONAL DENSITY FLUCTUATIONS, HELIOSPHERIC CURRENT SHEET AND CORONAL STREAMERS

Although much is known about the properties of density-fluctuations near the Sun, a critical characteristic that has not been determined in the past is the level of relative or fractional density fluctuations  $\delta n_e/n_e$  (Ref. 13), which is important for understanding the nature and role of the density fluctuations in the expansion of the solar wind (Ref. 50,51). Knowledge of relative density fluctuations also has relevance when density fluctuations inferred from radio scintillation and scattering measurements are used as a proxy for density (Ref. 10,35,52-55).

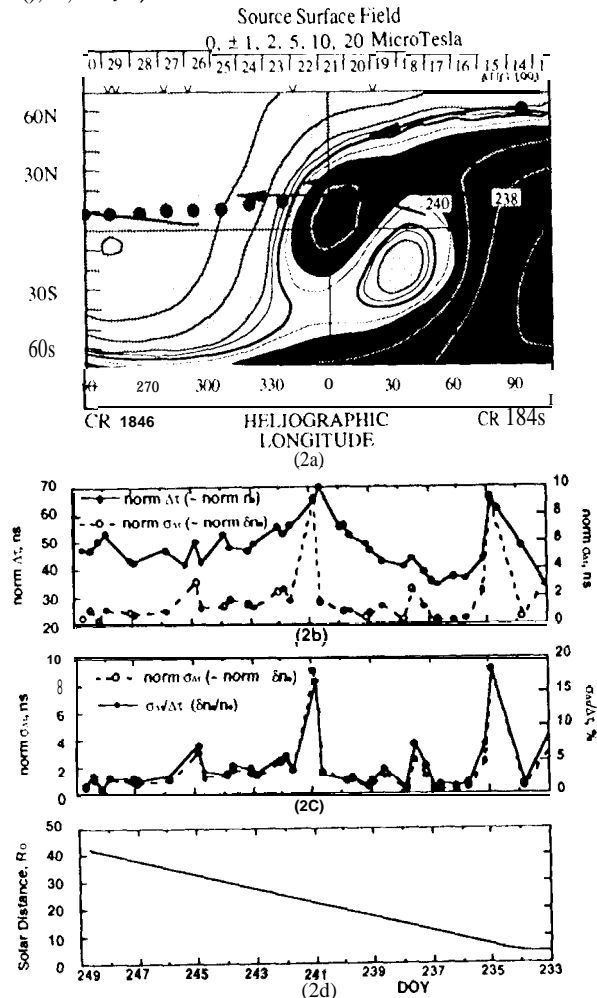


Figure 2. (a) Closest approach points (dots) of radio path projected onto coronal magnetic field map, (b) normalized time delay  $\Delta\tau$  (~normalized  $n_e$ ) and normalized time delay scintillation  $\sigma\Delta\tau$  (~normalized  $\delta n_e$ ), (c) normalized  $\sigma\Delta\tau$  (~normalized  $\delta n_e$ ) and ( $\delta n_e/n_e$ ), and (d) radial distance in  $R_0$  (from Ref. 56).

The first investigation of  $\delta n_e/n_e$  has been carried out using 10-min dual-frequency (wavelengths of 13.1 and 3.6 cm) measurements of time delay or ranging by Ulysses in August 1991 (Ref. 56). Time delay, or ranging, measures path-integrated electron density or total electron content, but to a good approximation it is proportional to electron density  $n_e$  at the closest approach point of the radio path (Ref. 42).

Shown in Fig. 2a is the Wilcox Observatory contour map of coronal magnetic field strength at 2.5 R<sub>⊙</sub> during the 1991 Ulysses radio measurements as adapted from Solar Geophysical data (Ref. S7). The solid dots represent the closest approach points of the Ulysses radio path on the denoted days of year (DOY), and hence indicate the corresponding approximate regions probed. Selected actual radio path segments near the closest approach points for a few days are also shown.

Mean values ( $\Delta\tau$ ) and standard deviations ( $\sigma\Delta\tau$ ) ~ proportional to density and density fluctuations, respectively - have been computed over periods typically 5-10 hours long. To remove the dependence on heliocentric distance, the measurements of time delay have been scaled to 1 AU according to the radial dependencies of R-1<sup>42</sup> as determined in Ref. 42. The standard deviations of time delay have also been scaled according to the radial dependence of R-1<sup>5</sup>, as has been observed in equivalent Doppler scintillation measurements near the Sun (Ref. 58).

The time histories of normalized  $\Delta\tau$  and  $\sigma\Delta\tau$  in nanoseconds are displayed in Fig. 2b. For convenience of comparison with the coronal field maps, the time axis has been reversed and displayed in such a manner that DOY lines up approximately with the corresponding dots in Fig. 2a. Corresponding heliocentric distances are shown in Fig. 2d, indicating that the Ulysses measurements took place inside 40 R<sub>⊙</sub>.

The density profile in Fig. 2b exhibits peaks near the neutral line, which are the apparent extensions of coronal streamers that have also been observed by *in situ* plasma measurements surrounding sector boundaries at 1 AU (Ref. 59,60). While the profiles of  $\delta n_e$  for the frequency band of  $-5 \times 10^{-5}$  -  $8 \times 10^{-4}$  Hz in Fig. 2b follows the same general pattern as  $n_e$ , the variations of  $\delta n_e$  are distinctly more abrupt and significantly greater (larger than an order of magnitude for  $\delta n_e$  vs less than a factor of 2 for  $n_e$ ). This is also demonstrated in the plot of  $\delta n_e/n_e$  in Fig. 2c showing variations of 1-20%. As with density fluctuations in the higher frequency band  $3 \times 10^{-3}$  -  $5 \times 10^{-2}$  Hz (periods of 10 scc to 3 rein) observed by Pioneer Venus (Ref. 5), density fluctuations in the lower frequency band are highest near the neutral line where the solar wind is slow, and lowest far from the neutral line where the solar wind is fast. These results reinforce the fact that the density spectrum near the Sun is not represented by a single spectrum (Ref. 16,18) but depends strongly on proximity to the neutral line (Ref. 6) as observed by *in situ* measurements

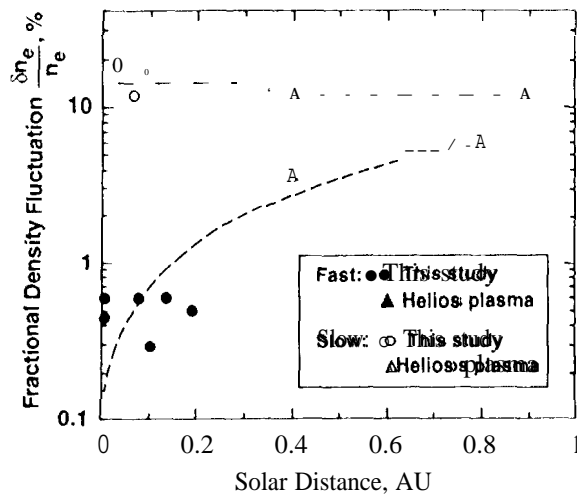


Figure 3.  $\delta n_e/n_e$  for spatial wavenumber  $K = 1.4 \times 10^6 \text{ km}^{-1}$ . Solid and hollow circles are Ulysses ranging measurements; solid and hollow triangles Helios *in situ* plasma measurements (from Ref. 56).

beyond 0.3 AU (Ref. 61) and meter wavelength IPS measurements (Ref. 19) of fast and slow solar wind. The similarity between Ulysses ranging measurements of low-frequency fluctuations and Pioneer Venus Doppler scintillation measurements of high-frequency fluctuations is also consistent with the broadband nature of increase in power spectrum of electron density fluctuations observed by Voyager scintillation measurements (Ref. 18) during the passage of 'transients,' some of which are probably associated with the heliospheric current sheet (Ref. 6)

Fig. 3 summarizes  $\delta n_e/n_e$  for spatial wavenumber  $K = 1.4 \times 10^6 \text{ km}^{-1}$  (5 hr fluctuation at a solar wind speed of 250 km/s) obtained for both slow and fast wind near 0.1 AU from the Ulysses radio measurements and at 0.4-0.9 AU from *in situ* Helios plasma measurements. In the slow wind,  $\delta n_e/n_e$  is essentially independent of heliocentric distance, while in the case of the fast wind, it is a factor of about 30 lower than that of the slow wind inside 0.1 AU, and exhibits dramatic growth with heliocentric distance inside 0.3 AU. This latter result provides additional evidence for significant evolution of the solar wind inside 0.3 AU as first revealed by the Pioneer Venus Doppler scintillation measurements (Ref. 5), and supports current views of the evolution of MHD turbulence with solar wind expansion and the association of Alfvén waves with high speed streams based on fields and particles measurements made beyond 0.3 AU (Ref. 51,61,62). The remarkably low density fluctuations associated with the fast wind also strengthens the argument for the presence of magnetic field fluctuations and Alfvén waves in high speed streams deduced from Faraday rotation fluctuations observed near the Sun (Ref. 43).

Fig. 2c shows that normalized AT, and hence normalized  $n_e$ , approximately tracks variations in  $\delta n_e/n_e$ . This is apparently a consequence of the fact that  $n_e$  varies more slowly than  $\delta n_e$ , and implies that it is possible to

obtain information on variations in fractional density fluctuations even when only measurements of density fluctuations are available, such as in the case of Doppler scintillation (Ref. 5).

That regions of enhanced density fluctuations near or above the neutral line coincide with regions of enhanced density confirms earlier conclusions that they are the interplanetary manifestation of the heliospheric current sheet and extensions of coronal streamers (Ref. 6). While the regions of enhanced density fluctuations lie within those of enhanced density, they have boundaries that are distinctly more abrupt, suggesting the separation of solar wind of different solar origin and wind speed. Further study based on higher time resolution Doppler scintillation data in the frequency band of  $3 \times 10^3 - 5 \times 10^3 \text{ Hz}$  (periods of 10 sec to 3 min) (Ref. 63) shows that the width of the enhanced region is about  $1-2^\circ$ , indicating a probable correspondence to the extensions of coronal streamers observed in high-resolution coronal white-light pictures such as that presented in Ref. 64. Furthermore, comparison of measurements obtained from successive solar rotations but with increasing heliocentric distance, reveals that near the Sun and within 0.3 AU, the structure inside the enhanced region is spatially coherent. These observations, therefore, provide the first evidence of the filamentary nature of the extensions of coronal streamers. These results also show for the first time that *in situ* measurements beyond 0.3 AU of compressive fluctuations in the slow wind of time scale about a couple of hours and faster (Ref. 61, 62, 65) are of coronal origin and are quasi-stationary. They bear the imprint of their solar source before being deformed by dynamic interaction during passage from the Sun.

Motivated by the Doppler scintillation results of the near-Sun solar wind, density fluctuations based on ISEE 3 plasma measurements in the range 10 reus to 1 hr have been investigated in the following solar wind flows at 1 AU: coronal hole, interstream, plasma sheet, coronal mass ejection, and interaction region (Ref. 60). While less extreme because of evolution with heliocentric distance, the ISEE 3 results confirm the interpretation of large-scale variations in density fluctuations observed by radio scintillation measurements inside 0.2 AU. The highest levels of absolute density fluctuations  $\sigma_N/\langle N \rangle$  and fractional density fluctuations  $\sigma_N/\langle N \rangle$  from the ISEE 3 study are found ahead of and in the plasma from coronal mass ejections, with the maximum values occurring between the associated interplanetary shocks and the driver gas. For the quasi-stationary solar wind, absolute and fractional density fluctuations and their variability are highest in the plasma sheet in which the heliospheric current sheet is embedded, and lowest in the high-speed coronal hole flow.

The results of a superposed epoch analysis of 18 HCS crossing events is presented in Fig. 4 for the interval  $\pm 3$  days either side of the boundary epoch,  $V$  is solar wind speed and  $B$  magnetic field. Similar superposed epoch studies of  $N$ ,  $V$ , and temperature  $T$ , have been presented

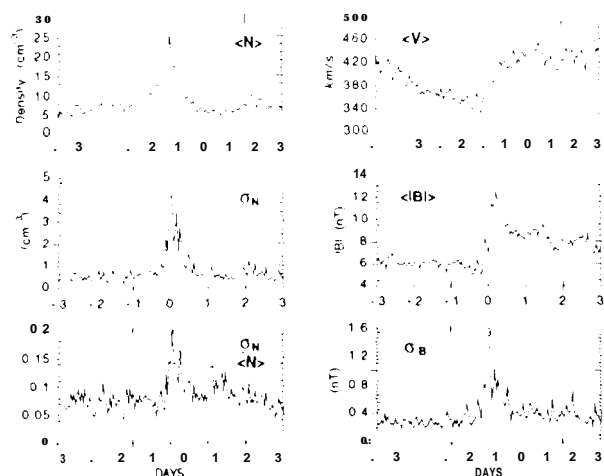


Figure 4. Superposed epoch study of ISEE-3 observations  $\pm 3$  days either side of the HCS (from Ref. 60).

(Ref. 66) but the results of  $\sigma_N$  have not. Near the Sun, the HCS is located in the dense, low-speed wind associated with the coronal streamer belt, which is surrounded by higher speed flows (Ref. 67). As the solar wind structure evolves with increasing distance, the compression ridge on the leading edge of the following high-speed stream gradually overtakes the HCS, causing the high fields seen just after the zero epoch. The velocity and field profiles show that, on the average for these 18 events, the leading edge of the following high speed stream has just passed over the HCS at the time it was observed. The density profile is narrower and less asymmetric than the field profile because of the intrinsic high density of the heliospheric plasma sheet. At 1 AU, there is a broad spike in  $\sigma_N$  at zero epoch, but it probably has contributions from both leading-edge compression and intrinsic variability of solar origin. The results in Fig. 4 have been compared and show good agreement with Doppler scintillation measurements near 1 AU (Ref. 63), providing further support for the filamentary nature of the extensions of coronal streamers.

The ISEE-3 study shows that coronal hole flow has the lowest levels of density and lowest levels of absolute and fractional density fluctuations. Further insight into measurements that sense density fluctuations are provided in Fig. 5 showing the comparison of enhancements in levels of density, and absolute and fractional density fluctuations over those of coronal hole flow for other types of solar wind. These results confirm what has been generally observed by comparing Doppler scintillation and in-situ plasma measurements of interplanetary shocks (Ref. 36), and time-delay and time-delay scintillation measurements of heliospheric current sheets shown in Fig. 2 – that the contrast in  $\sigma_N$  between various solar wind flows is not only high, but considerably higher than that of density. Closer to the Sun and before evolution with solar wind expansion, contrasts are even greater leading to prominent signatures for both coronal mass ejections and heliospheric current sheets. These results clearly

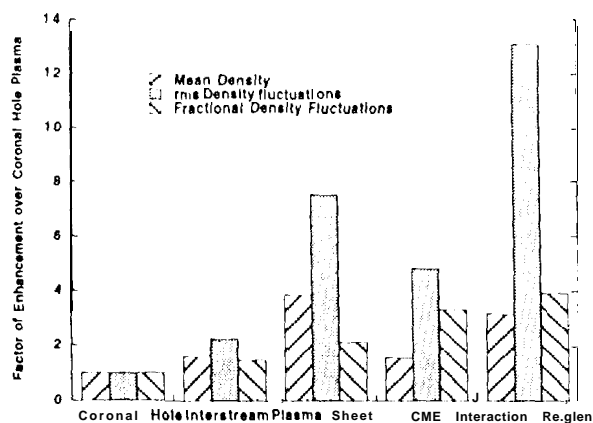


Figure 5. Ratios of mean density, density fluctuations, and fractional density fluctuations for various types of solar wind flow to the values in coronal hole flow (from Ref. 60).

demonstrate the advantages of using measurements that sense density fluctuations rather than density as tracers of solar wind flows with differing origins on the Sun and as detectors of propagating interplanetary disturbances.

#### V CORONAL MASS EJECTIONS AND INTERPLANETARY SHOCKS

Although Fig. 1 shows that scintillation transients are closely associated with white-light measurements of coronal mass ejections, scintillation measurements are more sensitive to CMEs because they sense density fluctuations rather than density. The extent of this increased sensitivity is demonstrated in Fig. 6 showing the factors of enhancement of Doppler scintillation transients. While factors of enhancement are typically 3-5 in the case of white-light CMEs (which as radio measurements are path-integrated measurements of electron density), they are strikingly greater in Doppler scintillation measurements, in some cases exceeding 50.

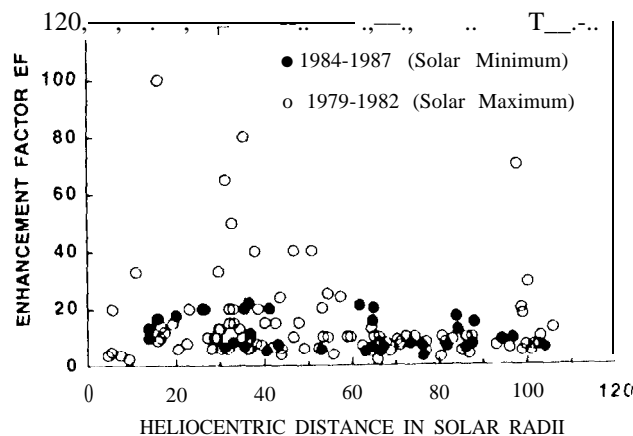


Figure 6. Distribution of factor of enhancement (EF) of Doppler scintillation transients over heliocentric distance (from Ref. 37).

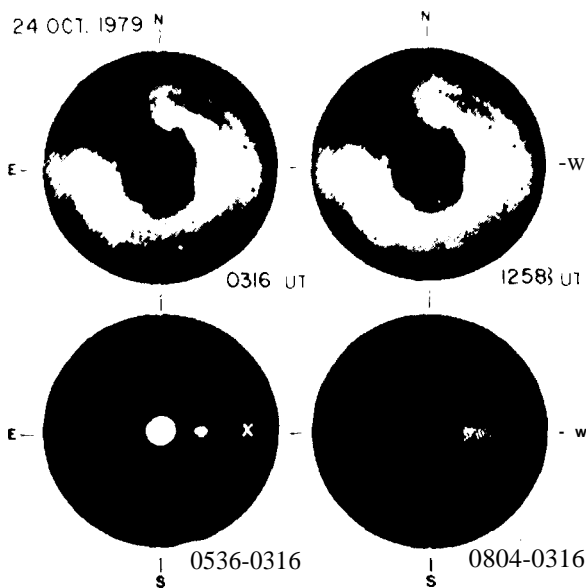


Figure 7. Solwind coronal images on 24 October 1979. See text for explanation (from Ref. 38).

There have been few opportunities for simultaneous measurements of CMEs, mainly because of the paucity of scintillation measurements near the Sun, but one instance did occur with Helios 2 spectral broadening and Solwind white-light coronagraph measurements [Woo et al., 1982]. The coronal images of the October 24, 1979 CME are shown in Fig. 7. The upper images were taken at 0316 and 1258 UT while the lower ones are difference images formed by subtracting the images at 0536 and 0804 UT from that at 0316 UT to show the changes that had taken place in the coronal intensity. The west limb brightening is always present during 0316-0804 UT. The Helios 2 raypath, which is in the ecliptic plane off the west limb of the Sun, moves towards the Sun at the rate of 25 km/s. "X" in the 0536-0316 UT difference image marks the location of the Helios 2 raypath at 0536 UT. Comparison with the time series of spectral broadening bandwidth shows that the delay in CME arrival is at least one hour. Thus, the compressive density fluctuations associated with this CME, and possibly representing the front of a shock, do not coincide with the white-light front, but precede it. This result is consistent with phase measurements of another shock on August 18, 1979 showing that mean density peaks well behind the shock front sensed by density fluctuations (Ref. 30), and poignantly demonstrates the benefits of conducting measurements that sense density fluctuations at the same time as white-light measurements. Joint measurements would also shed light on the outstanding question about forerunners (Ref. 68).

With the high level of density fluctuations following interplanetary shocks and the wide dynamic range of Doppler scintillation, it is now clear why Doppler scintillation measurements have served so well in accurately determining interplanetary shock crossings near the Sun. This unique ability has been used in conjunction with simultaneous white-light observations

of CMEs and *in situ* plasma measurements beyond 0.3 AU to obtain definitive measurements of interplanetary shock propagation and evolution inside 0.3 AU (Ref. 31). Shown in Fig. 8 are shock velocity profiles based on Solwind white-light coronagraph, Helios 1 plasma, and radio scintillation measurements by Voyager 1 (VI), Pioneer Venus (PV) and Pioneer 11 (P11) for nine shocks. These results, which are further supported by multi-spacecraft scintillation measurements (Ref. 69), show that substantial deceleration of fast shocks (speeds exceeding about 1000 km/s) takes place near the Sun, and that the amount of deceleration increases with shock speed. Alternately, the range of shock velocities inside 0.3 AU is significantly greater than those near Earth orbit. If the shocks are being driven to the point where deceleration begins, then the results in Fig. 8 imply that the slower shocks are being driven farther out than the fast shocks. On the basis of conventional MHD in the solar wind, the velocity profiles suggest that the fast shocks behave more like blast waves, while the slow

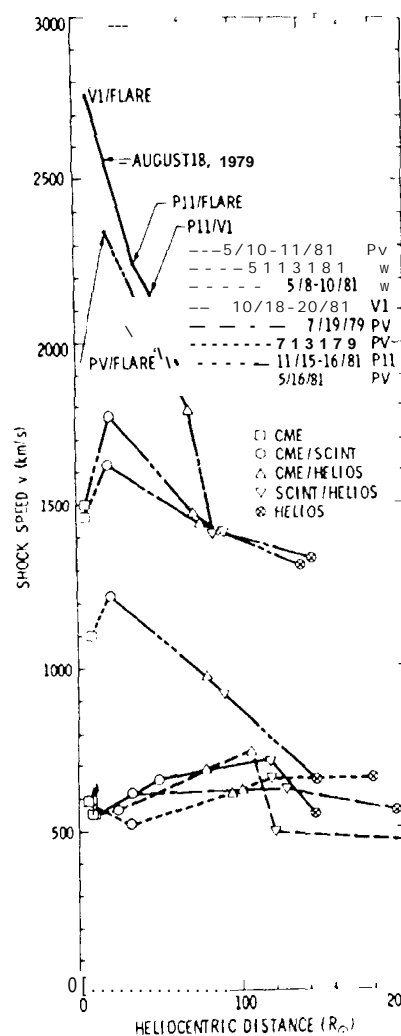


Figure 8. Velocity profiles for eight shocks observed by Solwind white-light, Helios plasma and Voyager 1 (V1), Pioneer Venus (PV) and Pioneer 11 (P11) Doppler scintillation measurements (from Ref. 31).

ones more like piston-driven waves (Ref. 70-72), These results suggest that the fast and rapidly decelerating shocks are associated with regions of very energetic and active solar flares, while the shocks with relatively low speeds, which may decelerate or move uniformly through the interplanetary medium, are associated with events characterized by the eruption and ejection of cool filamentary material from coronal quiescent regions (Ref. 73).

## VJ. OPPORTUNITIES FOR FUTURE SPACECRAFT RADIO SCINTILLATION OBSERVATIONS

The new developments described above underscore the urgency for simultaneous radio scintillation measurements that would complement both SOHO white-light corona graph and Yohkoh soft X-ray measurements, and significantly benefit the study of fine-scale structure and coronal mass ejections near the Sun. S-band (13 cm wavelength) radio scintillation measurements have been made since 1992 by Galileo and will continue during future superior conjunctions (Ref. 74,75) Cassini, which will be launched in 1997, will be invaluable because its radio system will have coherent radio signals in three bands: S- X- and Ka-bands (13, 3.6 and 1 cm wavelengths).

An unprecedented opportunity will arise with the ICE spacecraft during the SOHO era, as illustrated in ICE'S fixed Sun-earth line plot shown in Fig. 9. The region probed corresponds to the closest approach point. Unlike scintillation measurements in the past, the unusual ICE trajectory will allow ICE to probe the solar wind at near constant heliocentric distance inside 0.3 AU for prolonged periods during 1996-1998. Extensive high time resolution Doppler scintillation measurements at the same time as SOHO white-light coronagraph observations, which will observe the 'corona' out to  $30R_{\odot}$ , will therefore be possible.

## VII. SUMMARY AND CONCLUSIONS

Radio propagation experiments of the solar wind, actively pursued over the last forty years, have provided essentially all of the measurements of solar wind properties inside 0.3 AU. Because of the sparsity of measurements and the dominance of radial variation, they have often been limited to determining the heliocentric (but sometimes also latitudinal and/or solar cycle) dependence of density, density fluctuations and solar wind speed, with little progress in understanding the consequences of solar phenomena. Doppler scintillation and spectral broadening measurements, conducted with coherent spacecraft radio sources and possessing wide dynamic range and high time resolution, have made a significant difference. A global picture of the near-Sun solar wind consequences of solar phenomena is emerging from these measurements, one that relates and unifies results from centimeter ranging

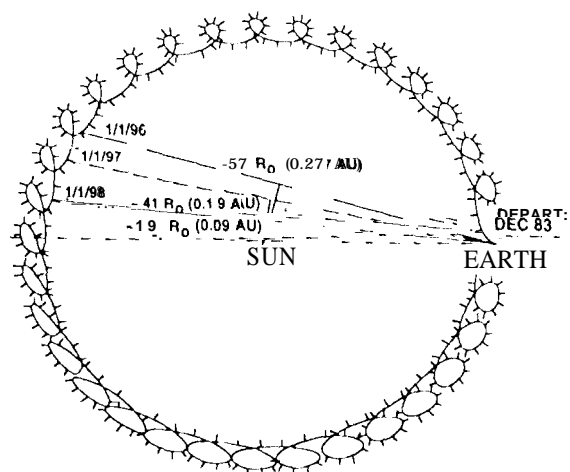


Figure 9. ICE trajectory relative to fixed Sun-Earth line in the ecliptic plane during 1983-2014. Lines indicate raypaths on January 1 of 1996, 1997 and 1998.

measurements in the vicinity of the Sun, meter wavelength IPS measurements beyond 0.5 AU, white-light coronagraph measurements, and *in situ* plasma measurements beyond 0.3 AU.

In the vicinity of the Sun, levels of compressive fluctuations produced and associated with CMEs are strikingly high but erode with heliocentric distance. Substantial deceleration of fast shocks (speeds exceeding  $\sim 1000$  km/s) takes place inside 0.3 AU, with the amount of deceleration decreasing with decreasing shock speed. There appears to be a tendency for fast shocks to be associated with solar flares, and slow shocks with eruptive prominences. The quasi-stationary structure overlying the neutral line near the Sun bears the imprint of its solar source, as it exhibits filamentary and fine structure before being deformed by dynamic interaction farther from the Sun. Far from the neutral line, and near the source region of the fast wind, where Alfvén waves are thought to dominate, density fluctuations are conspicuously slow and steady, but grow dramatically with heliocentric distance.

Comparison of density and density fluctuations, based on ranging measurements near the Sun and *in situ* plasma measurements at 1 AU, has clearly demonstrated the distinct advantages of density fluctuations (observed by scintillation measurements) over density (observed by ranging and white-light measurements) as tracers of solar wind flows from differing solar origins and as detectors of CMEs. The high sensitivity to quasi-stationary structure and dynamic phenomena make simultaneous scintillation measurements indispensable when probing the solar wind with other radio measurements such as Faraday rotation (Ref. 76).

Finally, taking full advantage of the new developments summarized in this paper by conducting simultaneous radio scintillation measurements with the SOHO corona graph during upcoming opportunities with

Galileo, Cassini and ICE is of paramount importance, as they will inevitably yield further details about the interplanetary manifestation of solar events and structure near the source region of the solar wind.

#### ACKNOWLEDGMENTS

It is a pleasure to thank J. Armstrong, M. Bird, P. Gazis, D. Huddleston, M. Neugebauer and M. Pätzold for useful discussions and collaboration. I am also grateful to the Galileo, Pioneer Venus and Ulysses Projects, and the NASA Deep Space Network for acquisition of radio scintillation data, to C. Chang for computer support, to C. Copeland for assistance in the production of this paper, and to D. Lozinski for bringing to my attention the ICE opportunity. This paper describes research carried out at the Jet Propulsion Laboratory, California Institute of Technology, under a contract with NASA.

#### REFERENCES

1. Hewish A. 1972, Observations of the solar plasma using radio scattering and scintillation methods, in Solar Wind, NASA Spec. Publ. SP-308 p. 477
2. Jokipii J.R. 1973, Turbulence and scintillations in the interplanetary plasma, Ann. Rev. Astron. Astrophys. 11, 1
3. Coles W.A. 1993, Scintillation in the solar wind (11'S), in Wave Propagation in Random Media (Scintillation), SPIE p. 156
4. Woo R. 1993, Spacecraft radio scintillation and solar system exploration, in Wave Propagation in Random Media (Scintillation), SPIE p. 50
5. Woo R. and Gazis P.R. 1993, Large-scale solar-wind structure near the Sun detected by Doppler scintillation, Nature 366, 543
6. Woo R., Armstrong J.W. and Gazis P.R. 1994, Doppler scintillation measurements of the heliospheric current sheet and coronal streamers close to the Sun, Space Sci. Rev. in press
7. Hewish A. 1958, The scattering of radio waves in the solar corona, Mon. Not. R. Astro. Soc. 118, 534
8. Vitkevich V.V. 1961, Radio astronomical observations of moving plasma clouds in the solar supercorona, Sov. Astron. 4, 897
9. Erickson W. C.. 1964, The radio-wave scattering properties of the solar corona, Ap. J. 139, 1290
10. Newkirk Jr. G. 1967, Structure of the solar corona, Ann. Rev. Astron. Astrophys. 5, 213
11. Armstrong J. W., Colts W. A., Kojima M. and Rickett B.J. 1990, Observations of field-aligned density (fluctuations in the inner solar wind, Ap. J. 358, 685
12. Sakurai T., Spangler S.R. and Armstrong J.W. 1992, Very long baseline interferometer measurements of plasma turbulence in the solar-wind, J. Geophys. Res. 97, 17141
13. Bourgois G. and Colts W.A. 1992, Solar cycle changes in the turbulence level of the polar stream near the Sun, in Solar Wind Seven, eds. R. Schwenn and H. Marsch, Pergamon Press p. 155
14. Manoharan P.K. 1993, Three-dimensional structure of the solar wind: Variation of density with the solar cycle, Solar Phys. 148, 153
15. Lotova N.A. 1975, Current ideas concerning the spectrum of the irregularities in the interplanetary plasma, Sov. Phys.-Usp. 18, 292
16. Woo R. and Armstrong J.W. 1979, Spacecraft radio scattering observations of the power spectrum of electron density fluctuations in the solar wind, J. Geophys. Res. 84, 7288
17. Armand N. A., Efimov A.I. and Yakovlev O.I. 1987, A model of the solar wind turbulence from radio occultation measurements, Astron. Astrophys. 183, 135
18. Coles W.A., Liu W., Harmon J.K. and Martin C. I. 1991, The solar wind density spectrum near the Sun: Results from Voyager radio measurements, J. Geophys. Res. 96, 1745
19. Manoharan P. K., Kojima M. and Misawa H. 1994, The spectrum of electron-density fluctuations in the solar wind and its variations with solar-wind speed, J. Geophys. Res., in press
20. Woo R. and Goldstein R M 1994, Latitudinal variation of speed and mass flux in the acceleration region of the solar wind inferred from spectral broadening measurements, Geophys. Res. Letts 21, 85
21. Lallement R., Holzer T.E. and Munro R.H. 1986, Solar wind expansion in a polar coronal hole: Inferences from coronal white light and interplanetary Lyman alpha observations, J. Geophys. Res. 91, 675
22. Hewish A, Scott P.F. and Wills D. 1964, Interplanetary scintillation of small diameter radio sources, Nature 203, 1214
23. Ekers R.D. and Little L.T. 1971, The motion of the solar wind close to the Sun, Astron. Astrophys. 10, 310
24. Scott S.I., Colts W.A. and Bourgois G. 1983, Solar wind observations near the Sun using interplanetary scintillation, Astron. Astrophys. 123, 207

25. Armstrong J. W., Colts W. A., Kojima M. and Rickett B.J. 1986, Solar wind observations near the Sun, in *The Sun and the Heliosphere in Three Dimensions* (ed. R.G. Marsden, D. Reidel, p. 59
26. Colts W. A., Esser R., Løvhaug U.-P. and Markkanen J. 1991, Comparison of solar wind velocity measurements with a theoretical acceleration model, J. Geophys. Res. 96, 13849
27. Krrjima M. and Kakinuma T. 1990, Solar cycle dependence of global distribution of solar wind speed, Space Sci. Rev. 53, 173
28. Rickett B.J. and Coles W.A. 1991, Evolution of the solar wind structure over a solar cycle: interplanetary scintillation velocity measurements compared with coronal observations, J. Geophys. Res. 96, 1717
29. Rickett B.J., Disturbances in the solar wind from IPS measurements in August 1972, Solar Phys. 43, 237
30. Woo R., and Armstrong J.W. 1981, Measurements of a solar flare-generated shock wave at 13.1 R<sub>o</sub>, Nature 292, 608
31. Woo R., Armstrong J. W., Sheeley Jr. N. R., Howard R. A., Koomen M. J., Michels D.J. and Schwenn R. 1985, Doppler scintillation observations of interplanetary shocks within 0.3 AU, J. Geophys. Res. 90, 154
32. Tappin S. J., Hewish A, and Gapper G.R. 1983, Tracking a major interplanetary disturbance, Planet. Space Sci. 31, 1171
33. Watanabe T. and Schwenn R. 1989, Large-scale propagation properties of interplanetary disturbances revealed from IPS and spacecraft observations, Space Sci. Rev. S1, 147
34. Houminer Z. 1971, Corotating plasma streams revealed by interplanetary scintillation, Nature 231, 165
35. Ananthakrishnan S., Coles W.A. and Kaufman J.J. 1980, Microturbulence in solar wind streams, J. Geophys. Res. 85, 6025
36. Woo R, and Schwenn R. 1991, Comparison of Doppler scintillation and *in situ* spacecraft plasma observations of interplanetary disturbances, J. Geophys. Res. 96, 21227
37. Woo R. 1993, Solar cycle variation of interplanetary disturbances observed as Doppler scintillation transients, J. Geophys. Res. 98, 18999
38. Woo R., Armstrong J. W., Sheeley Jr. N. R., Howard R. A., Michels D.J. and Koomen M.J. 1982, Simultaneous radio scattering and white light observations of a coronal transient, Nature 300, 157
39. Esposito P.B., Eidenhofer P, and Lüneburg E. 1980, Solar corona electron density distribution, J. Geophys. Res. 85, 3414
40. Muhleman D.O. and Anderson J.D. 1981, Solar wind electron densities from Viking dual-frequency radio measurements, Ap. J. 247, 1093
41. Anderson J. D. et al. 1987, Radio range measurements of coronal electron densities at 13 and 3.6 cm wavelengths during the 1985 solar occultation of Voyager 2, Ap. J. 323, 1141
42. Bird M. K., Volland H., Pätzold M., Eidenhofer P., Asmar S.W. and Brenkle J.P. 1994, The coronal electron density distribution determined from dual-frequency ranging measurements during the 1991 solar conjunction of the Ulysses spacecraft, Astrophys. J. 426, 373
43. Hollweg J. V., Bird M. K., Volland H., Eidenhofer P., Stelzried C.T. and Seidel B.L. 1982, Possible evidence for coronal Alfvén waves, J. Geophys. Res. 87, 1
44. Zirker J. II. (ed. ) 1977, Coronal Holes and High Speed Wind Streams, Colorado Associated University Press
45. Hundhausen A.J. 1993, Size and locations of coronal mass ejections SMM observations from 1980 and 1984-1989, J. Geophys. Res. 98, 13177
46. Mendoza B. and Pérez-Enriquez R. 1993, Association of coronal mass ejections with the heliomagnetic current sheet, J. Geophys. Res. 98, 9365
47. Spangler S.R. 1992, Radio propagation experiments and remote measurement of interplanetary plasma turbulence, in Proceedings of the First SOL TIP Symposium, Astronomical Institute of the Czechoslovak Academy of Sciences p. 228
48. Harrison, R.A. 1990, The source regions of solar coronal mass ejections, Solar Phys. 126, 185
49. Lotova N. A., Investigation of the solar wind transonic region, Solar Wind Seven, COSPAR Colloquia Series 3, 217
50. Marsch E. 1991, MHD turbulence in the solar wind, in Physics of the Inner Heliosphere, Vol. 2, eds R Schwenn and E. Marsch, Springer, p. 159
51. Roberts D. A., and Goldstein M.I. 1991, Turbulence and waves in the solar wind, Rev. Geophys. 29, 932
52. Houminer Z. and Hewish A, 1974, Correlation of interplanetary scintillation and spacecraft plasma density measurements, Planet. Space Sci. 20, 1041

53. Tappin S.J. 1986, Interplanetary scintillation and plasma density, Planet. Space Sci. 34,93
54. Zwickl R., Hildner E., Bame S. J., Gosling, J.T. and Sofaly K. 1988, Relationship between solar wind density fluctuations and density at high frequency. EOS (abstract) 69, 1358
55. Woo R. and Gazis P.R. 1994, Mass flux in the ecliptic plane and near the Sun deduced from Doppler scintillation, Geophys. Res. Letts 21, 1101
56. Woo R., Armstrong J. W., Bird M.K. and Pätzold M. 1994, Variation of fractional electron density fluctuations near 0.1 AU from the Sun observed by Ulysses dual-frequency ranging measurements, Geophys. Res. Letts., submitted
57. Hoeksema J.T. and Scherrer P.H. 1986, The solar magnetic field - 1976 through 1985, Rep. UAG-94, World Data Cent. A for Sol. Terr. Phys. S
58. Woo, R. 1978, Radial dependence of solar wind properties deduced from Helios 1/2 and Pioneer 10/1 radio scattering observations, Astrophys. J. 219
59. Gosling J. T., Borrini G., Asbridge J. R., Bame S. J., Feldman W. C. and Hansen R. T. 1981, Coronal streamers in the solar wind at 1 AU, J. Geophys. Res. 86, 5438
60. Huddleston D. E., Woo R. and Neugebauer M. 1994, Density fluctuations in different types of solar wind flow at 1 AU and comparison with Doppler scintillation measurements near the Sun, J. Geophys. Res., submitted
61. Marsch E. and Tu C.-Y. 1990, Spectral and spatial evolution of compressible turbulence in the inner solar wind, J. Geophys. Res. 95, 11945
62. Bavassano B. 1994, Recent observations of MHD fluctuations in the solar wind, Ann. Geophys. 12,97
63. Woo R., Armstrong J. W., Bird M.K. and Pätzold M. 1994, Spatial structure in the extensions of coronal streamers near the Sun, J. Geophys. Res., in preparation
64. Koutchmy S. 1992 Streamer eclipse observations, in Coronal Streamers. Coronal Loops and Coronal and Solar Wind Composition, ESA SP-348 p. 73
65. Velli M. and Grappin R. 1993, Properties of the solar wind, Adv. Space Res. 13, 49
66. Borrini G., Gosling J. T., Bame S. J., Feldman W.C. and Wilcox J.M. 1981, Solar wind helium and hydrogen structure near the heliospheric current sheet: A signal of coronal streamers at 1 AU, J. Geophys. Res. 86, 4565
67. Gosling J. T., Borrini G., Asbridge J. R., Bame S. J., Feldman W.C. and Hansen R.T. 1981, Coronal streamers in the solar wind at 1 AU, J. Geophys. Res. 86, 5438
68. Jackson B.V. and Hildner E. 1978, [Forerunners: Outer rims of solar coronal transients, Sol. Phys. 60, 155
69. Woo R. 1988, A synoptic study of Doppler scintillation transients in the solar wind, J. Geophys. Res. 93, 3919
70. Hundhausen A.J. and Gentry R.A. 1969, Numerical simulation of flare-generated disturbances in the solar wind, J. Geophys. Res. 74, 2908
71. D'Uston C., Dryer M., Han S.M. and Wu S.T. 1981, Spatial structure of flare-associated perturbations in the solar wind simulated by a two-dimensional numerical MHD model, J. Geophys. Res. 86, 525
72. Smith Z. and Dryer M. [1990, MHD study of temporal and spatial evolution of simulated interplanetary shocks in the ecliptic plane within 1 AU, Solar Phys. 129, 387
73. Cane H. V., Kahler S.W. and Sheeley Jr. N.R. 1986, interplanetary shocks preceded by solar filament eruptions, J. Geophys. Res. 91, 13321
74. Howard H.T. et al. 1992, Galileo radio science investigations, Space Sci. Rev. 60, 565
75. Woo R. et al. 1992, Galileo radio scintillation and scattering measurements during and around the superior conjunction of January 22, 1992, EOS (abstract) 73, 238